A Factor Graph Based Indoor Localization Approach for Healthcare

A Factor Graph-Based Indoor Localization Approach for Healthcare

Shiyu Zheng, Ziheng Zhou, Qi Zhang,
Shanshan Zhang, Ao Peng, Lingxiang Zheng*
School of Informatics
Xiamen University
Xiamen, China
lxzheng@xmu.edu.cn

Huiru Zheng, Haiying Wang
School of Computing and Mathematics
University of Ulster
Belfast, United Kingdom
h.zheng@ulster.ac.uk

***Abstract*—In healthcare facilities, indoor localization technology has a broad range of applications. Traditional Pedestrian Dead Reckoning (PDR) and WiFi fingerprint-based methods each have their limitations. To address these challenges, this study introduces a multi-source fusion indoor localization system that uses a Factor Graph to integrate inertial positioning algorithms with WiFi fingerprint-based localization. The system processes accelerometer and gyroscope data using a data-driven PDR algorithm. For WiFi localization, considering that the extensive data collection required is a significant barrier to the deployment of WiFi-based localization methods, the proposed approach applies Gaussian process regression techniques to limited WiFi fingerprint data, significantly reducing initial deployment costs and enhancing accuracy. Finally, the entire system employs a Factor Graph for the integration of the data-driven PDR and WiFi fingerprint localization results. Experimental results show that, compared to using only inertial or WiFi data for localization, this method significantly improves localization accuracy. The findings suggest that this approach could promopt the utilization of indoor localization technology in healthcare facilities.**

Keywords: Indoor Positioning;fingerprint positioning; Factor Graph; Gaussian Process Regression

1. Introduction

Indoor positioning technology is increasingly finding applications across a variety of settings from shopping malls and airports to healthcare facilities. In the healthcare sector, accurately determining the locations of patients and healthcare professionals is important in the provision of high-quality medical services. However, conventional Global Navigation Satellite Systems (GNSS) are typically unavailable in indoor settings and, even if occasionally accessible, they provide highly unreliable positioning information. As a result, there is a growing need for specialized indoor positioning solutions in modern healthcare.

* *Corresponding author*
Email address: lxzheng@xmu.edu.cn (Lingxiang Zheng)

In such healthcare environments, the applications for indoor positioning are diverse. The quick and accurate identification of examination rooms or wards is not just a convenience but a necessity for patients, while healthcare providers need a reliable system to track locations for efficient care delivery. Especially for vulnerable populations like the elderly or those with cognitive impairments, robust monitoring and precise localization are of utmost importance [1]. However, achieving high-precision in indoor positioning systems for healthcare remains a challenging task, owing to a variety of factors such as cost, infrastructure limitations, and specific healthcare requirements.

Taking into account the widespread availability and cost-effectiveness of WiFi in healthcare settings, an integrated pedestrian indoor positioning system is proposed which combines an inertial data-driven Pedestrian Dead Reckoning (DPDR) algorithm with a WiFi Received Signal Strength Indicator (RSSI) positioning algorithm. The aim is to find a balanced intersection between accuracy, cost, and usability, particularly for certain healthcare applications. By enhancing positioning accuracy, there exists the potential to improve patient experiences, elevate the operational efficiency of healthcare institutions, and strengthen the capabilities of medical professionals in patient monitoring and care. Furthermore, the research contributes to the ongoing development of indoor positioning technology, broadening its applications beyond healthcare into diverse sectors.

The remainder of this paper is structured as follows. Section 2 provides an overview of related works. In Section 3, we elucidate the methodology of our proposed integration platform. Section 4 encompasses the presentation of our experiments and results. Lastly, Section 5 draws the paper to a conclusion.

2. Related work

In recent years, healthcare and the associated healthcare facility (HCF) location problems have become noticeably more critical and important to society [2]. This is particularly crucial for vulnerable populations, such as the elderly or individuals with cognitive impairments, where

robust monitoring and precise localization are of paramount importance. A study conducted by [3] explored various positioning techniques aimed at improving the accuracy of activity recognition for the elderly within their homes or in nursing facilities. Emphasis was placed on the significance of location information in understanding the contextual environment of users, ultimately providing assistance to enhance their quality of life. However, existing research has been limited by factors such as accuracy, complex models, limited coverage, and high costs, making it challenging to establish a standardized solution.

In current indoor environments, WiFi signals are virtually ubiquitous, sparking significant research interest in WiFi-based indoor positioning technologies. Of these, WiFi fingerprint-based localization stands out for its low deployment costs and relatively high positioning accuracy. However, its accuracy is closely tied to the quality of WiFi fingerprint databases, which can be labor-intensive and resource-consuming to create such a detailed and high quality database.To address this challenge and reduce costs, numerous researchers have focused on fingerprint augmentation. For instance, one approach [4] involves enhancing the training of deep learning models by augmenting fingerprint data through the random extraction of Received Signal Strength (RSS) information from reference points (RPs). Another approach [5] utilizes a Multivariate Gaussian Process Regression (MGPR) model to predict RSS values for unexplored locations within multi-story buildings, thereby generating additional fingerprints. These innovative strategies aim to enhance the quality and diversity of WiFi fingerprint data while mitigating the associated resource burden. Despite these advancements in fingerprint augmentation techniques, challenges remain in achieving localization error stabilization and trajectory smoothness in WiFi fingerprint-based systems. The complexities of indoor environments and the quality of collected data can significantly affect the performance of localization algorithms. These factors can introduce inconsistencies and fluctuations in the positioning results, making them less reliable over time. In practical scenarios, even with sophisticated augmentation methods, issues such as unstable error margins and abrupt location jumps are yet to be fully addressed. Therefore, while these strategies enhance the quality and density of WiFi fingerprint data, they do not entirely resolve the inherent limitations of WiFi fingerprint-based localization.

Another important method for indoor localization is Pedestrian Dead Reckoning (PDR), which analyzes sensor data from accelerometers and gyroscopes to estimate the user's spatial coordinates. Traditional PDR methods, especially those involving foot-mounted sensors, rely on distinct zero-velocity points to truncate errors. However, when these inertial sensors are positioned on the upper body—a scenario commonly encountered in healthcare settings—the absence of such zero-velocity points, along with the presence of noise, presents challenges for accurate displacement estimation. To tackle these issues, current research predominantly focuses on data-driven PDR approaches where sensors are mounted on the upper body. For instance, IONet [6] employs a neural network model to directly extract coordinate transformations from Inertial Measurement Units (IMU). In a similar data-driven vein, RoNIN uses deep neural networks to predict human motion velocity, offering a different approach from IONet, which models the transformation of inertial sensor data into displacement. Generally speaking, DPDR techniques that employ deep neural network models hold a distinct advantage over traditional methods. However, they also come with limitations. Notably, inertial-based PDR algorithms are a form of relative positioning that calculates displacement with respect to a starting point. This approach is susceptible to accumulating errors, which can become significant over extended periods of operation.

Both WiFi fingerprint-based and inertial data-based PDR localization schemes have their limitations. To address these challenges, this study proposes a hybrid indoor positioning system that employs a factor graph to integrate inertial positioning algorithm with WiFi fingerprint algorithm. The system utilizes inertial sensors, including accelerometers and gyroscopes, for the implementation of a data-driven PDR algorithm. When processing WiFi RSSI data, the proposed method applies Gaussian process regression technique to the limited WiFi fingerprint data, thereby significantly reducing initial deployment costs and enhancing accuracy. The factor graph is employed for the seamless integration of both inertial and WiFi-based algorithms. Factor Graph Optimization (FGO) offers advantages over the widely-used Kalman filtering for data fusion because it encompasses all historically observed measurements, which are used in various navigation systems [7]. This approach aims to enhance the robustness and stability of the positioning system, thereby meeting the healthcare requirements for indoor localization technology.

3. Method

The framework of the proposed factor graph-based indoor localization approach is presented in Figure 1. This system comprises several components: the Data-Driven Pedestrian Dead Reckoning algorithm, which processes inputs from accelerometers and gyroscopes; the WiFi fingerprinting method that involves training to generate the fingerprint database and then is augmented via Gaussian Process Regression; the floor detection module that utilizes barometer clustering and WiFi localization results; and finally, the fusion algorithm based on the Factor Graph, which consolidates the outputs of the aforementioned methods to deliver accurate and robust indoor localization results.

3.1. Inertial Data-Driven Pedestrian Dead Reckoning Algorithm

For the traditional research of indoor positioning using inertial sensors, the acceleration data and angular velocity data collected by inertial sensors are processed. The processing formula is shown in equation (1)(2)

$$\mathbf{a} = \hat{\mathbf{a}} + \mathbf{n}_a \tag{1}$$

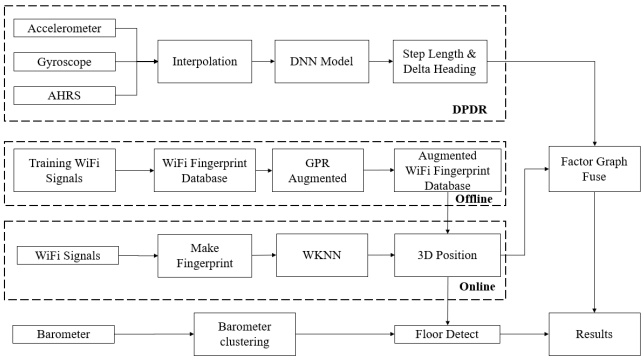

Figure 1. System Framework Diagram

$$\omega = \hat{\boldsymbol{\omega}} + \mathbf{n}_\omega \tag{2}$$

$\hat{\mathbf{a}}$ and $\hat{\omega}$ represent the true values of acceleration and angular velocity respectively, while $\mathbf{n}_a$ and $\mathbf{n}_\omega$ represent the noise data introduced by the acceleration and gyroscope respectively. The acceleration and the angular velocity can be represented as a 3×1 vector respectively, as shown in equation(3)

$$a = \begin{pmatrix} a_x + n_a \\ a_y + n_a \\ a_z + n_a \end{pmatrix} \quad \omega = \begin{pmatrix} \omega_x + n_\omega \\ \omega_y + n_\omega \\ \omega_z + n_\omega \end{pmatrix} \tag{3}$$

The direction cosine matrix $\mathrm{C}_b^n(t)$ is used to represent the transformation of the coordinate system, which is expressed as equation(4), and can be rotated through $\boldsymbol{\Omega}_b$, which can be shown as equation(5)

$$\mathbf{C}_b^n(t) = \mathbf{C}_b^n(t-1)\boldsymbol{\Omega}_b \tag{4}$$

$$\boldsymbol{\Omega}_b = \begin{pmatrix} 0 & -\omega_x - n_\omega & \omega_y + n_\omega \\ \omega_z + n_\omega & 0 & -\omega_x - n_\omega \\ -\omega_y - n_\omega & \omega_x + n_\omega & 0 \end{pmatrix} \tag{5}$$

Meanwhile, in the discrete time environment, if a small time step Δt is given, the update process of the direction cosine matrix $\mathrm{C}_b^n(t)$ can be approximated by the following equation (6).

$$\mathbf{C}_b^n(t + \Delta t) \approx \mathbf{C}_b^n(t)(I + \boldsymbol{\Omega}_b \Delta t) \tag{6}$$

Using this process, the direction is transformed into the navigation frame. At the same time, the position and speed of the pedestrian can be derived from the following formula. The velocity can be integrated by equation(7), and the contribution of gravity to acceleration can be eliminated by equation(8)

$$\mathbf{v}_n(t) = \mathbf{v}_n(t-1) + \mathbf{a}_n(t-1)dt \tag{7}$$

$$\mathbf{a}_n(t-1) = \mathbf{C}_b^n(t-2)\mathbf{a}_b(t-1) - \mathbf{g}_n \tag{8}$$

Finally, the location information can be obtained by equation(9) (10).

$$\mathbf{d}_n(t) = \mathbf{d}_n(t-1) + \Delta d. \tag{9}$$

$$\Delta d = \mathbf{v}_n(t-1)dt + \frac{1}{2}\mathbf{a}_n(t-1)dt^2 \tag{10}$$

According to the above formula, it can be concluded that for the traditional PDR method, the errors introduced by it will accumulate continuously in the integration process, affecting the calculation accuracy of the navigation position. Therefore, considering the powerful data processing capability of deep neural network, a data-driven scheme is adopted to replace the traditional PDR integration process, so as to reduce personnel drift.

Aiming at the problems existing in the traditional integration process of PDR, we discuss the modeling. First, We focus on speed.

For velocity, our modeling process can be shown in equation (11)

$$\mathbf{v}_n(t) = \mathbf{v}_n(t-1) + \Delta v \tag{11}$$

The speed value of the current moment is equal to the speed value of the previous moment plus the speed increment value.

For displacement, from equation(9), our modeling process can be shown by equation(12).

$$\Delta d = f(X;\theta) \tag{12}$$

θ Represents the parameters used by the model. And $X = [x_1, x_2, ..., x_n]$ represents all inertial navigation measurements in a time window, where $x_1 = [a_1, w_1]$

Through the analysis of the above model, it can be seen that whether the speed or position is modeled, the input data is sequential, so the neural network can be used for effective processing. For relatively short walk sequences, Recurrent Neural Network(RNN) is used to process input sequences effectively, considering the memory ability of RNN. For the path with long walking time or complex trajectory, the feature extraction capability of Convolutional Neural Network(CNN) can be used to extract the feature values in the sequence to process the sensor data more effectively.

3.2. WiFi fingerprint positioning with Gaussian Process Regression

Common WiFi fingerprinting methods impose specific requirements on the density and quality of the fingerprint database. Generally, a higher fingerprint density leads to improved localization accuracy. However, achieving a higher WiFi fingerprint density necessitates substantial upfront data collection costs. Consequently, this study employs Gaussian Process Regression to delineate the spatial relationship between Access Points (APs) and WiFi fingerprints, thereby facilitating a certain degree of augmentation to the WiFi fingerprint database.

Each WiFi fingerprint is represented as a vector composed of RSS values, denoted as $\boldsymbol{y} = [RSS_1, RSS_2, \ldots, RSS_M]$, where M is the total number of detected APs in the entire dataset. Additionally, we define the position vector for RPs as $c = [x, y, z]$, where x and

y represent coordinates on a two-dimensional plane, and z represents the height of the floor, all measured in meters.

For all RSS vectors $y_1, y_2, ..., y_N$ in set Y, and $c_1, c_2, ..., c_N$ in set C, where N denotes the number of collected fingerprints, the mapping relationship between location and RSS vectors is represented by the function $f(\cdot)$:

$$Y = f(\boldsymbol{C}) + \eta \tag{13}$$

The noise η is typically assumed to be independent and identically distributed Gaussian noise with a mean of zero and a variance of σ_n^2, and can be expressed as $\eta \sim N(0, \sigma_n^2)$.

To address this mapping, it is assumed that all RSS vectors within the investigated indoor region follow a multivariate Gaussian process with multiple high-dimensional joint Gaussian distributions. Gaussian processes are characterized by the mean function

$$m(\boldsymbol{C}) = \mathbb{E}[f(\boldsymbol{C})] \tag{14}$$

and the covariance function

$$\operatorname{cov}(f(\mathbf{c}_i), f(\mathbf{c}_j)) = \mathbb{E}[(f(\mathbf{c}_i) - m(\mathbf{c}_i))(f(\mathbf{c}_j) - m(\mathbf{c}_j))] \tag{15}$$

describing the relationships among these random variables. Here, $\mathbb{E}$ represents the mathematical expectation. We represent the Gaussian process as $\mathcal{GP}()$, and $f(\boldsymbol{C})$can be defined as:

$$f(\boldsymbol{C}) \sim \mathcal{GP}(\mu(\boldsymbol{C}), \operatorname{cov}(\boldsymbol{C})) \tag{16}$$

Furthermore, through the utilization of the kernel trick, the covariance function does not necessitate the computation of a complex $f(c)$:

$$\begin{aligned} \operatorname{cov}(f(\mathbf{c}_i), f(\mathbf{c}_j)) &= \mathbb{E}[(f(\mathbf{c}_i) - m(\mathbf{c}_i))(f(\mathbf{c}_j) - m(\mathbf{c}_j))] \\ &= k(\mathbf{c}_i, \mathbf{c}_j) \end{aligned} \tag{17}$$

The covariance matrix K can then be expressed as:

$$K = \begin{bmatrix} k(c_1, c_1) & k(c_1, c_2) & \cdots & k(c_1, c_N) \\ k(c_2, c_1) & k(c_2, c_2) & \cdots & k(c_2, c_N) \\ \vdots & \vdots & \ddots & \vdots \\ k(c_N, c_1) & k(c_N, c_2) & \cdots & k(c_N, c_N) \end{bmatrix} \tag{18}$$

As RPs are typically sparsely distributed within indoor environments, it can be challenging to construct reliable fingerprints in areas with sparse WiFi signal coverage. To enhance the fingerprints in these unknown regions, we introduce additional RPs, denoted as $C^* = [C_1^*, C_2^*, \ldots, C_{N^*}^*]^T$, for predicting the corresponding WiFi fingerprints. Here, N^* represents the number of newly added RPs. According to the characteristics of Gaussian process regression, the RSS vectors in the original dataset, denoted as Y, and the RSS vectors to be inferred, denoted as Y^*, should also follow a joint multivariate Gaussian distribution defined by the following equations:

$$\begin{bmatrix} Y \\ Y^* \end{bmatrix} \sim \mathcal{N}\left(\begin{bmatrix} m(C) \\ m(C^*) \end{bmatrix}, \begin{bmatrix} K(C,C)_{N\times N} & K(C,C^*)_{N\times N^*} \\ K(C^*,C)_{N^*\times N} & K(C^*,C^*)_{N^*\times N^*} \end{bmatrix} \right) \tag{19}$$

The posterior distribution $p(y^*|y)$can be expressed as:

$$\begin{aligned} y^*|y \sim \mathcal{N}(K(C^*,C)K(C^*,C)^{-1}y), \\ K(C^*,C^*) - K(C^*,C)K(C^*,C)^{-1}K(C,C^*)) \end{aligned} \tag{20}$$

Thus, it is possible to compute the posterior mean and covariance of the observed RSS vectors to formulate a predictive model for generating novel RSS vectors at unexplored RPs..

Furthermore, the kernel function $k(c_i, c_j)$ plays a pivotal role in Gaussian processes, capturing the relationships between RSS vectors and their corresponding RPs. In complex, large indoor environments, single kernels may not perform as effectively as composite kernels. Therefore, we choose to employ a compound kernel function that combines the Matern and Rational Quadratic (RQ) kernels, which were demonstrated to perform best in the context of this study as presented in [8]. The Matern kernel is defined as follows:

$$\begin{aligned} k_{Matern}(c_i, c_j) = \\ \frac{1}{\Gamma(\nu)2^{\nu-1}} \left(\frac{\sqrt{2\nu}}{l} d(c_i, c_j) \right)^{\nu} K_\nu \left(\frac{\sqrt{2\nu}}{l} d(c_i, c_j) \right) \end{aligned} \tag{21}$$

Here $d(c_i, c_j) = \sqrt{(c_i - c_j)^T (c_i - c_j)}$ is the Euclidean distance; ν represents the smoothness of the function; l is the length scale; $K_\nu(\cdot)$ and $\Gamma(\cdot)$ represent the gamma function and modified Bessel function.

The rational quadratic kernel can be described as:

$$k_{RQ}(\boldsymbol{c}_i, \boldsymbol{c}_j) = \left(1 + \frac{d(\boldsymbol{c}_i, \boldsymbol{c}_j)^2}{2\alpha l^2} \right)^{-\alpha} \tag{22}$$

Where α signifies the shape parameter. Therefore, the compound kernel design in our case is structured as follows:

$$k_{compound} = \mu * k_{Matern} + \nu * k_{RQ} \tag{23}$$

Here, μ and ν are the weighting parameters. All the aforementioned hyperparameters can be optimized by minimizing the negative log marginal likelihood.

After fingerprint augmentation, the fingerprint matching algorithm did not exhibit substantial differences. Consequently, for fingerprint matching, we have employed the WKNN algorithm, known for its ease of implementation and portability, and have utilized the Euclidean distance as the metric for inter-fingerprint distance computation.

$$d_i = \sqrt{\sum_{j=1}^{n} \left(rssi'_{ij} - rssi_{ij} \right)^2} \tag{24}$$

3.3. Factor Graph-Based Data Fusion

Factor Graph is a graph structure used to represent probabilistic models, particularly well-suited for the factorization and inference processes within probabilistic graphical models.

Factor Graphs consist of two types of nodes: variable nodes and factor nodes. Variable nodes represent optimization variables, while factor nodes represent constraint conditions. Factor Graph optimization involves determining a

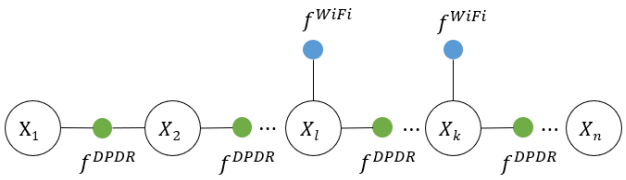

Figure 2. Factor Graph fusion structure

combination of variable values that satisfy the constraints specified by all factor nodes. It is a graphical representation used to address inference problems within probabilistic graphical models, providing a clear depiction of the dependencies between variables and the composition of probability factors.

In the process of localization, we often need to estimate a set of state variables X based on a given set of measurements Z Assuming a Markov model, this conditional probability density function can be represented using the formula:

$$P(X|Z) = \prod_{i=1}^{k} \frac{P(z_i|x_i)P(x_i|x_{i-1}, u_i)}{P(z_i)} P(x_0) \tag{25}$$

Here,z_i represents the measurement results observed at epoch i (e.g., WiFi measurements), x_i represents the system state at time i, and u_i represents control inputs (e.g., PDR measurements).

The purpose of the Factor Graph framework is to find the most probable posterior state of the unknown state variables X given the measurement history. Therefore, the essence of the localization problem is a Maximum A Posteriori (MAP) problem.

$$\hat{X} = \arg\max P(X|Z) = \arg\max \prod_{i=1}^{k} P(z_i|x_i)P(x_i|x_{i-1}, u_i) \tag{26}$$

In Factor Graph, all of these likelihood and transition probabilities can be viewed as a factorization of the global probability:

$$\hat{X} = \arg\max \prod_{j=1}^{n} f(x_j) \tag{27}$$

In the example presented in this paper, the factor graph model can be represented as $G = (F, X, E)$, where X represents the set of variable nodes ($x_i \in X$), depicted as circles in Figure 2, representing the state information at various time instances. F represents the set of factor nodes ($f_j \in F$), denoted by solid points, which are cost functions capturing the discrepancies between predictive and measurement information. The core objective of factor graph fusion is to find the optimal estimate $\hat{X}$ that minimizes the error of the cost function $f(x)$.

Each factor simulates a constraint and must incorporate a measure of uncertainty. The most common model is Gaussian noise:

$$P(z_i|x_i) \propto \exp\left(-\frac{1}{2}\|h_i(x_i - z_i)\|^2 \nabla_i\right) \tag{28}$$

$$P(xi|x_{\boldsymbol{i}-1}) \propto \exp\left(-\frac{1}{2}\|\Phi_i(x_{\boldsymbol{i}-1} - x_i)\|^2 \Omega_i\right) \tag{29}$$

Here, the function $\Omega_i(\cdot)$ describes the relationship between the previous state x_{i-1} and x_i, while the function $h_i(\cdot)$ represents the relationship between state x_i and measurement z_i. The covariance matrices are denoted by ∇_i and Ω_i. By taking the negative logarithm and removing the factor of 1/2, the problem is transformed into the minimization of an error function, effectively a nonlinear least-squares problem:

$$\hat{X} = \arg\min\left(\sum_{i=1}^{k} \|\Phi_i(x_{i-1}) - x_i\|^2_{\Omega_i} + \sum_{i=1}^{k} \|h_i(x_i) - z_i\|^2_{\nabla_i}\right) \tag{30}$$

DPDR factor The DPDR factor is a binary factor associated with the states at two adjacent time instances, used to describe measurements between states. In DPDR, it is associated with the changes in position and heading between two time instances.

$$s_k^{DPDR} = \begin{bmatrix} \Delta L_k \\ \Delta \psi_k \end{bmatrix} \tag{31}$$

where ΔL_k and $\Delta \psi_k$ denote the change of the position and heading at epoch k , respectively. Hence, the error function for the observation values of the DPDR factor, denoted as e^{DPDR}, is expressed as follows:

$$e_k^{DPDR} = \begin{bmatrix} \|p_k - p_{k-1}\| \\ \Psi_k^q - \Psi_{k-1}^q \end{bmatrix} - \begin{bmatrix} \Delta L_k \\ \Delta \psi_k \end{bmatrix} \tag{32}$$

Based on the DPDR constraint, the sum of squared errors can be expressed as follows.

$$F_{DPDR}(\cdot) = \sum_i \|e_k^{DPDR}\|^2_{\Omega_k^{DPDR}} \tag{33}$$

Ω_k^{DPDR} represents the covariance matrix associated with the DPDR localization performance. This matrix is constant and is determined based on the accuracy of the data-driven PDR method. In this paper, the covariance matrix is represented as follows:

$$\Omega_k^{DPDR} = \begin{bmatrix} 2^2 & 0 \\ 0 & 0.5^2 \end{bmatrix} \tag{34}$$

WiFi Factor This factor represents the constraint imposed by the WiFi measurements:

$$\left\|e_k^{WiFi}\right\|^2_{\sum_k^{WiFi} = \|X_k - WiFik\|^2_{\sum_k^{WiFi}}} \tag{35}$$

Therefore, based on the two aforementioned cost functions, the non-linear least-squares problem can be formulated as:

$$\hat{X} = \arg\min \left(\sum_{i=1}^{k} \left[\left\| e_i^{DPDR} \right\|^2_{\Omega_k^{DPDR}} + \left\| e_i^{WiFi} \right\|^2_{\sum_i^2 WiFi} \right] \right) \tag{36}$$

To address the least-squares problem, considering the favorable convergence properties of the Levenberg-Marquardt (LM) algorithm, the LM algorithm is employed to obtain the optimal solution.

4. Experiment Evaluation

4.1. Dataset

In order to make the experiment more relevant to healthcare facilities,our dataset selection was primarily guided by the following considerations:

1. **Accumulative IMU Errors:** Recognizing that errors in the IMU tend to accumulate over time, we deliberately selected datasets with longer time durations. This choice allowed us to better capture the cumulative impact of these errors.

2. **Inhomogeneous WiFi Signals in Large Buildings:** To replicate the non-uniform distribution of WiFi signals within expansive structures, we focused on datasets collected within multi-story, large-scale edifices. This approach enabled us to offer a more realistic portrayal of the WiFi signal conditions encountered in practical real-world applications.

3. **Complex Indoor Environments:** To more effectively illustrate WiFi signal attenuation, blockages, and multipath effects in indoor settings, we selected datasets from complex indoor environments, as opposed to simple and open spaces.

In line with these criteria, we opted for the publicly available dataset from IPIN2023 Competition [9]. This dataset was meticulously gathered within the Museum for Industrial Culture situated in Nuremberg, Germany. The museum is about 3,500 m^2 , has a main Ground Floor (Level 0) and a large open area in the Basement (Level -2). There is also a small Mezzanine, which we consider as Level -1 in this dataset. During the data collection phase, two distinct participants collected all the logfiles and trials for training, testing and scoring. While both participants adhered to identical data collection protocols, subtle variations in their natural poses, smartphone handling techniques, and step lengths were introduced. The smartphones employed were the Samsung A5 2017 (SM-A520F running Android 8.0.0) and the Samsung S7 (SM-G930F also running Android 8.0.0). This selection ensures the diversity and complexity of the dataset, thus facilitating a comprehensive evaluation of our system's performance.

4.2. WiFi fingerprint positioning

In WiFi preprocess work, the primary focus is on the creation of a fingerprint database. In this process, RSS values that are not present are set to 110 dB, and access points (APs) are subjected to filtering. This filtration includes the removal of APs with excessively low occurrence frequencies to ensure the manageability of fingerprint size. Additionally, APs with abnormally high occurrence frequencies are filtered to maintain the accuracy of the fingerprints. Then the RSS data is normalized with minmax normalization to establish the mapping of fingerprints to position coordinates. After generating the fingerprint database, it can be seen from the figure 3 that the RP points are relatively sparse and uneven, so we use the GPR approach mentioned in 3.2 to augment the fingerprint database, which is mainly realized with the Gpytorch [10] package.In real-time localization, we use WKNN to obtain position.

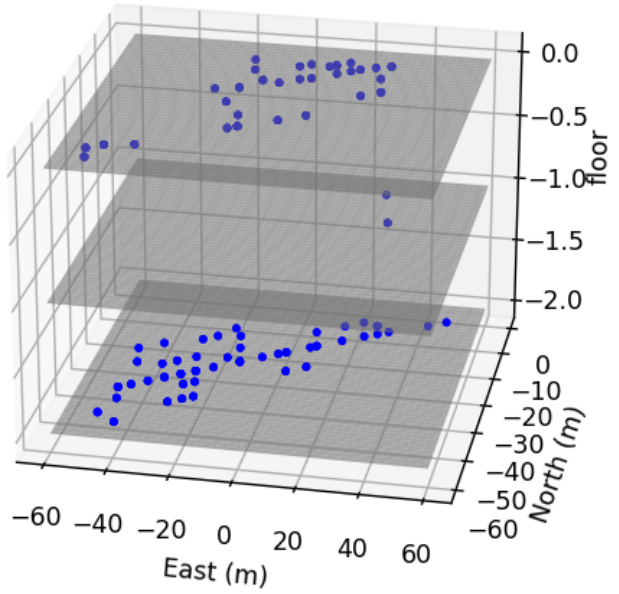

Figure 3. Distribution of wifi RPs on different floors

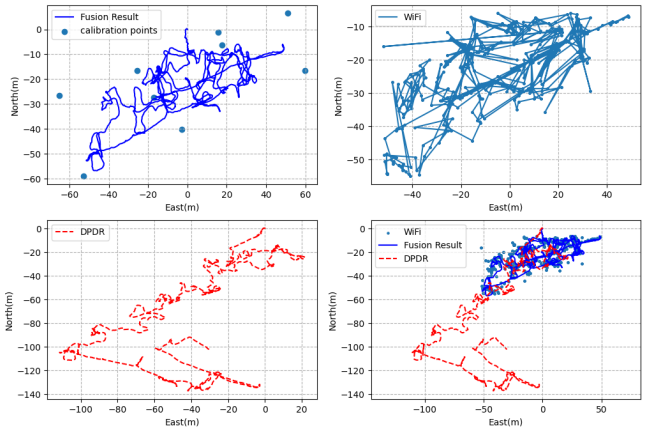

Figure 4. 2D Trajectories of different method

4.3. Data-driven Pedestrian Dead Reckoning

For the DPDR part, it is essential to perform uniform interpolation on sensor data of varying frequencies, interpolating them into a 200Hz data stream. Additionally, the data needs to be rotated based on the positional information obtained from smartphone sensors before being input into the network for further processing.

Since the frequency of each sensor is not consistent, we are required to interpolate the data during preprocessing, and in this experiment we uniformly interpolate the data to 200hz.In order to remove the effect of posture on acceleration, the data needs to be rotated according to the position information obtained from the smart phone sensors.For comparison purposes, we use publicly available algorithms [11].

This study primarily focuses on fusion algorithms, and hence, the DPDR component employs the RONIN [11]. During data processing, interpolation is applied to sensor data with varying frequencies. The data is uniformly interpolated to a standardized frequency of 200Hz. Subsequently, the data is rotated based on the pose information obtained from mobile sensors before being fed into the network. The output comprises velocity, which is further integrated to derive step length and heading.

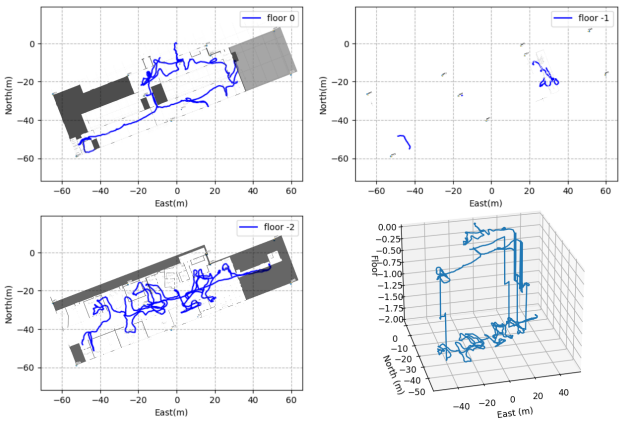

Figure 5. 2D Trajectories of different floors and 3D trajectories

4.4. Floor Detection

Our floor detection method mainly based on air pressure difference between the average air pressure value of the current sliding window and the initial calibrated air pressure. Therefore, we need to first cluster and analyze the barometer data of different floors based on the training data, so as to obtain the threshold value of the relative difference between different floors. The average value of the barometric pressure in the sliding window is taken in the detection, and the floor is switched if the barometric pressure difference with the initial barometric pressure reaches the threshold, and the detection is assisted by combining the floor data obtained from WiFi positioning. This method achieves 100% correctness among 69 ground truth points provided in the dataset.

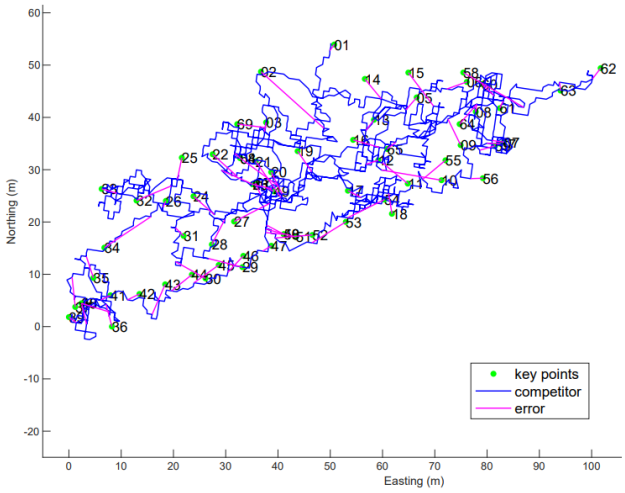

Figure 6. Results of the IPIN competition Track 3

4.5. Evaluation

In the experimental phase, we evaluated the performance of the system and tested it using the scoring file provided with the dataset, which was recorded for a total duration of about 30 minutes of time, covering mainly three floors. While the system was running, we continuously received data streams from the sensors and fed them into the network every 0.5 seconds in order to obtain the location of the DPDRs and then insert them into the factor graph implemented by GTSAM [12]. When we have WiFi data available, we generate the current WiFi fingerprint and use the WKNN algorithm to compare it with the fingerprints in the fingerprint database to obtain the localization result of the WiFi fingerprints, and then input this result into the factor graph. Finally, we extract the results of the factor graph for analysis.

As shown in the Figure 4, we observe that pure DPDR performs relatively poorly under long complex trajectories. In the second half of the trajectory, we notice that the trajectory deviates significantly from the expected path due to the cumulative error of heading drift. On the other hand, pure WiFi localization also shows some challenges in these cases. Due to the discontinuity of the WiFi signals, we observe that the WiFi localization data show intermittency and there are still significant outliers at some of the more distant WiFi signal points.

When using factor graph fusion, the continuity of DPDR compensates for the lack of WiFi intermittency while the cumulative error of DPDR is corrected by the WiFi factor, and the use of historical information by the factor graph makes the outliers of the WiFi localization results further reduce the negative impact of the results. In order to present the experimental results more clearly, we plot the trajectories of

different floors separately in Figure 5. Combining the maps shows that the fused results also have a better performance in turning to complex trajectories.

This trajectory dataset consists of 69 ground truth points, as depicted in the figure. Error calculations based on these ground truth points are presented in the Figure 7 and TABLE 1. The average errors for pure DPDR and pure WiFi fingerprint-based localization are 74.44 meters and 9.78 meters respectively. Fusion of both data sources significantly enhances the localization accuracy, resulting in an average positioning error of 5.60 meters, with 75% of errors within 6.25 meters. This result won second place in IPIN2023 Competition Track 3.

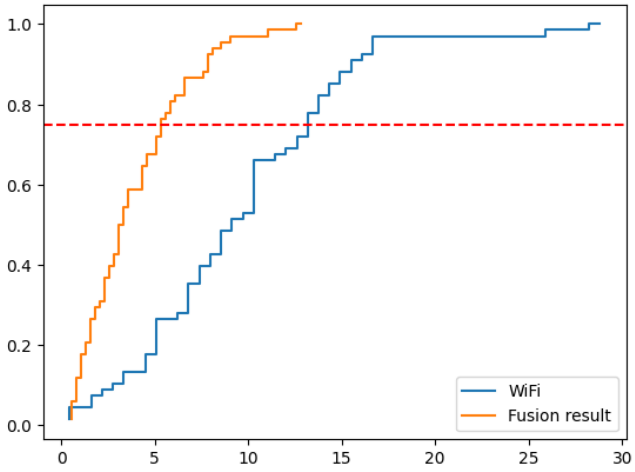

Figure 7. CDF of WiFi and fusion results

Method	RMSE	MEDIAN	90th perc	75th perc
FGO	5.60	4.31	7.93	6.25
DPDR	74.44	77.10	98.52	127.98
WiFi	9.78	9.36	15.63	13.42

TABLE 1. ACCURACY OF DIFFERENT POSITIONING METHODS

5. Conclusion

Considering the widespread availability of WiFi in healthcare facilities, this study explores the method to enhance the traditional WiFi fingerprint localization algorithm by integrating it with a data-driven PDR algorithm. A Factor Graph serves as the cornerstone for fusing the advantages of data-driven PDR and WiFi-based methods, thereby addressing the inherent weaknesses of WiFi localization. The incorporation of Gaussian process regression further augments the efficiency and accuracy of WiFi fingerprint localization by reducing initial deployment costs which is always a barrier to deploy the WIFI localization system. Experimental results indicate that the proposed approach outperforms traditional WiFi fingerprint localization algorithm. However, it should be noted that further research is needed to fully validate the effectiveness and scalability of this approach. Overall, this research represents an attempt to enhance the robustness and efficiency of indoor localization systems, and it encourages further exploration of the usability of the technique in healthcare facilities.

Acknowledgments

This work was supported by Science and Technology Major Program of Fujian Province (No. 2022HZ026007).

References

[1] A. Al-Molegi and A. Martínez-Ballesté, "Safemove: monitoring seniors with mild cognitive impairments using deep learning and location prediction," *Neural Computing and Applications*, vol. 34, no. 19, pp. 16 785–16 803, 2022.

[2] A. Ahmadi-Javid, P. Seyedi, and S. S. Syam, "A survey of healthcare facility location," *Computers & Operations Research*, vol. 79, pp. 223–263, 2017.

[3] L. Bibbò, R. Carotenuto, and F. Della Corte, "An overview of indoor localization system for human activity recognition (har) in healthcare," *Sensors*, vol. 22, no. 21, p. 8119, 2022.

[4] R. S. Sinha and S.-H. Hwang, "Improved rssi-based data augmentation technique for fingerprint indoor localisation," *Electronics*, vol. 9, no. 5, p. 851, 2020.

[5] Y. Dong, T. Arslan, Y. Yang, and Y. Ma, "A wifi fingerprint augmentation method for 3-d crowdsourced indoor positioning systems," in *2022 IEEE 12th International Conference on Indoor Positioning and Indoor Navigation (IPIN)*. IEEE, 2022, pp. 1–8.

[6] C. Chen, X. Lu, A. Markham, and N. Trigoni, "Ionet: Learning to cure the curse of drift in inertial odometry," in *Proceedings of the AAAI Conference on Artificial Intelligence*, vol. 32, no. 1, 2018.

[7] W. Wen, T. Pfeifer, X. Bai, and L.-T. Hsu, "Factor graph optimization for gnss/ins integration: A comparison with the extended kalman filter," *NAVIGATION: Journal of the Institute of Navigation*, vol. 68, no. 2, pp. 315–331, 2021.

[8] W. Sun, M. Xue, H. Yu, H. Tang, and A. Lin, "Augmentation of fingerprints for indoor wifi localization based on gaussian process regression," *IEEE Transactions on Vehicular Technology*, vol. 67, no. 11, pp. 10 896–10 905, 2018.

[9] T.-S. J. (2023) Datasets and supporting materials for the ipin 2023 competition track 3 (smartphone-based, off-site). Zenodo. [Online]. Available: https://doi.org/10.5281/zenodo.8362205

[10] J. R. Gardner, G. Pleiss, D. Bindel, K. Q. Weinberger, and A. G. Wilson, "Gpytorch: Blackbox matrix-matrix gaussian process inference with gpu acceleration," *arXiv preprint arXiv:1809.11165*, 2018.

[11] S. Herath, H. Yan, and Y. Furukawa, "Ronin: Robust neural inertial navigation in the wild: Benchmark, evaluations, & new methods," in *2020 IEEE International Conference on Robotics and Automation (ICRA)*. IEEE, 2020, pp. 3146–3152.

[12] frank dellaert, "Factor graphs and gtsam: A hands-on introduction," 2012.